

Inelastic Deuteron Scattering and (d,p) Reactions from Isotopes of Ti. II. $Ti^{47}(d,p)Ti^{48\dagger}$

P. D. BARNES AND C. K. BOCKELMAN
Yale University, New Haven, Connecticut

AND

OLE HANSEN
Institute for Theoretical Physics, University of Copenhagen, Copenhagen, Denmark

AND

A. SPERDUTO
Massachusetts Institute of Technology, Cambridge, Massachusetts

(Received 28 December 1964)

The (d,p) reaction from a target of isotopically separated Ti^{47} has been studied at 6-MeV bombarding energy. Proton spectra were recorded simultaneously at 24 scattering angles with an over-all energy resolution of 15 keV by means of a broad-range, multiple-gap, heavy-particle spectrograph. Fifty-five proton groups, corresponding to levels in Ti^{48} , were observed. To forty of these (d,p) groups, transition strengths and values of the orbital angular momenta of the transferred neutrons were assigned by means of a distorted-wave analysis of the differential cross sections. A sum-rule analysis shows that virtually all of the $1f_{7/2}$, $2p_{3/2}$, and $2p_{1/2}$ single-particle strengths and 25% of the $1f_{5/2}$ strength were observed. A level scheme for Ti^{48} is proposed and the available spectroscopic information on the low-lying levels is discussed in terms of current nuclear models.

I. INTRODUCTION

THE present article is the second in a series of papers¹ concerned with (d,p) and (d,d') reactions from isotopes of Ti. It reports on the results from the reaction $Ti^{47}(d,p)Ti^{48}$.

Fifty-five levels in Ti^{48} were identified in the present experiment, and the corresponding proton angular distributions were measured. The over-all energy resolution was 15 keV, and the bombarding energy was 6.00 MeV. Forty of the observed angular distributions could be analyzed in the distorted-wave Born approximation to yield values of the orbital angular momenta of the transferred neutrons (l_n values) and absolute transition strengths $(2J_f+1)S_{lj}^{J_f}$, where J_f designates the final-state spin, l the l_n value, j the total angular momentum of the neutron, and S the spectroscopic factor which measures the overlap between the target ground state plus a neutron and the final state.

The present experiment extends the region of excitation energies studied in earlier $Ti^{47}(d,p)Ti^{48}$ experiments²⁻⁴ to 8 MeV. On the basis of a shell-model sum-rule analysis of the presently observed transition strengths, this region covers the whole of the $1f_{7/2}$, $2p_{3/2}$, $2p_{1/2}$ strengths, and part of the $1f_{5/2}$ strength.

The target ground state of the present experiment,

[†] This work was supported in part by the U. S. Atomic Energy Commission with funds provided under Contract AT(30-1)2098 with the Massachusetts Institute of Technology, and under Contract AT(30-1)2627 with Yale University.

¹ P. D. Barnes, C. K. Bockelman, O. Hansen, and A. Spurduto, Phys. Rev. **136**, B438 (1964) on the $Ti^{50}(d,p)Ti^{51}$ reaction, and to be published on the $Ti^{49}(d,p)Ti^{50}$ reaction.

² M. M. Bretscher, J. O. Alderman, A. Elwyn, and F. B. Shull, Phys. Rev. **96**, 103 (1954).

³ N. I. Zaika and D. F. Nemets, Izv. Akad. Nauk SSSR, Ser. Fiz. **24**, 865 (1960).

⁴ J. L. Yntema, Phys. Rev. **131**, 811 (1963).

Ti^{47} , has, outside a Ca^{48} core, two $f_{7/2}$ protons and three $f_{7/2}$ neutron holes coupled to a spin of $\frac{5}{2}$. This state cannot be described as a single-particle state of a spherical nucleus. The Ti^{48} ground state is particularly simple, it being a $0+$ state of a configuration consisting of two $f_{7/2}$ protons and two $f_{7/2}$ neutron holes. As, furthermore, spins and parities of a number of low-lying Ti^{48} states are known experimentally, the deuteron stripping reaction connecting the Ti^{47} ground state and states of Ti^{48} can yield valuable information on the coupling schemes for these two nuclei. A detailed comparison of the spectroscopic evidence on Ti^{48} (from earlier works as well as the present work) with predictions of current nuclear models is presented in Sec. V. Special emphasis is given to the recent model of McCullen, Bayman, and Zamick.⁵ Preceding sections cover the experimental results and analysis (Sec. II), a comparison with other experiments and the proposal of a level scheme for Ti^{48} (Sec. III), and a comparison of the experimental transition strengths with the shell-model sum rules (Sec. IV).

II. EXPERIMENTAL TECHNIQUES, RESULTS, AND ANALYSIS

A detailed account of the experimental procedures and the distorted-wave Born approximation (DWBA) analysis has been given previously.¹ In this section, we shall therefore describe only those points that are unique for the Ti^{47} bombardments.

The observed angular distribution of deuterons scattered elastically from Ti^{47} at 6.00 MeV is shown in Fig. 1 (circles). Also shown are the distributions calculated from the optical model using the average Ti potential $B4$ (dashed curve), and the best-fit potential $B3/1$ (full

⁵ J. D. McCullen, B. F. Bayman, and L. Zamick, Phys. Rev. **134**, B515 (1964).

curve). The parameters of the potentials are given in Ref. 1.

As can be seen from Fig. 1, the average potential (*B4*) gives nearly as good a fit to experiment as does the *B3/1* potential. In Fig. 2, $l_n=1$ (*d,p*) angular distributions of $Q=7$ MeV, computed from the same proton potential (given in Ref. 1) and from the *B4* and *B3/1* deuteron potentials, respectively, are shown. The area under the *B4* curve is 1.05 times the area under the *B3/1* curve.

The DWBA predictions used for determining spectroscopic factors were computed for a target mass of 49.

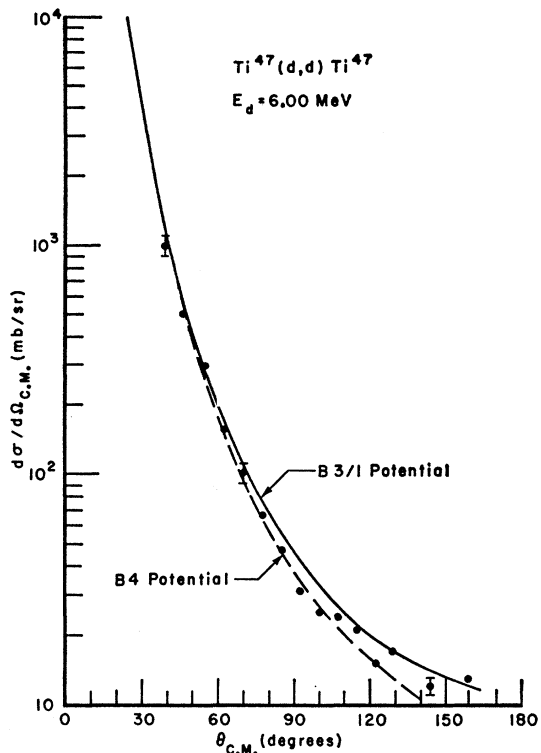


FIG. 1. The circles show the results of the measurement of the $Ti^{47}(d,d)Ti^{47}$ angular distribution at 6.00 MeV. The full-drawn curve is generated from the Ti^{47} *B3/1* potential (see Ref. 1) and the dashed curve from the *B4* average *Ti* potential. The vertical bars represent typical experimental errors.

The variation with mass of the computed distributions is slight and actually partially compensates the effect introduced by using the average *B4* potential instead of the best-fit potential. Throughout the present work we have used the average *B4* potential for target mass 49 without any corrections.

The quality of the fit of DWBA predictions to experiment may be judged from Figs. 3 through 17 which present a selection of the measured distributions.⁶

In order to obtain spectroscopic factors, the theo-

⁶ Copies of the complete set of experimental data may be obtained from the authors.

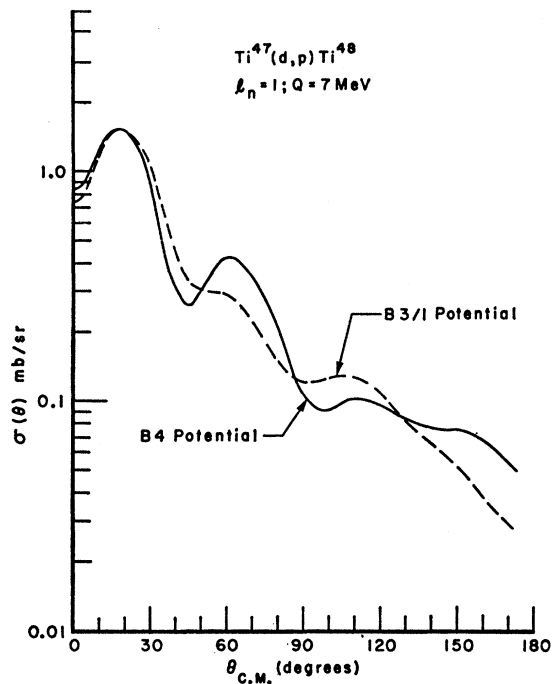


FIG. 2. Predicted angular distributions for $Ti^{47}(d,p)Ti^{48}$, $Q=7$ MeV and $l_n=1$. The full-drawn curve was generated by the *B4* average *Ti* deuteron potential, the dashed curve from the *B3/1* Ti^{47} deuteron potential. In both cases the same proton potential was used (see Ref. 1). The main difference in the predicted distributions is the shape of the second maximum. The areas under the curves are identical within 5%. (See also the discussion in the text.)

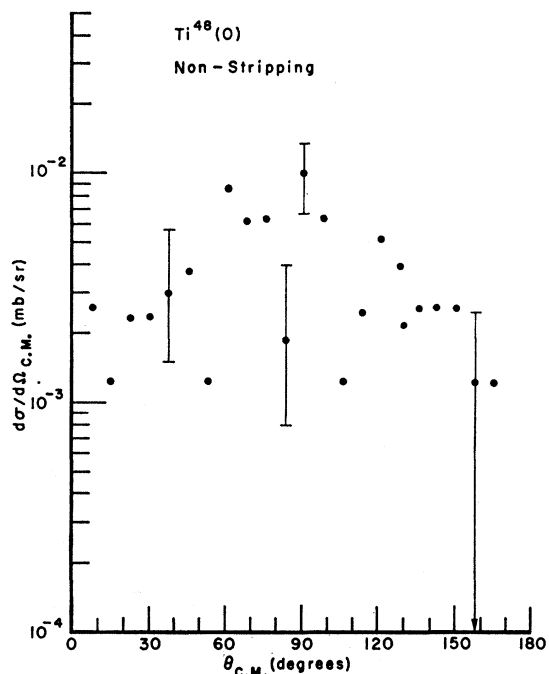


FIG. 3. Experimental proton distribution observed for the transition to the Ti^{48} ground state. The distribution is of "nonstripping" character.

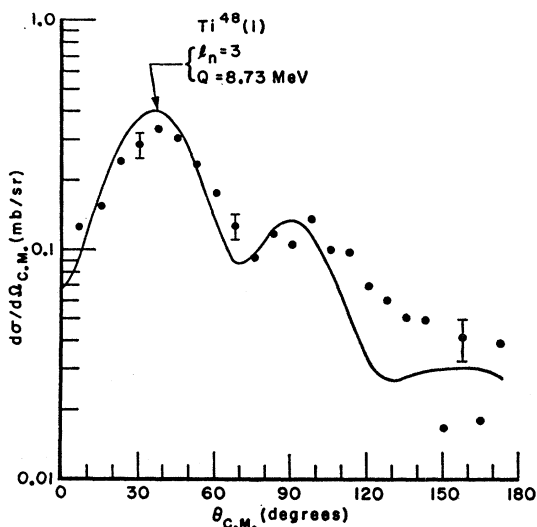


FIG. 4. Experimental distribution (circles) for the $Ti^{47}(d,p)$ transition to $Ti^{48}(1)$. Typical errors are indicated by the vertical bars. The curve is the $l_n=3$ distribution predicted by DWBA calculations from potential $B4$ at $Q=8.73$ MeV normalized to the same area as experimentally observed. There is no evidence for $l_n=1$ admixtures.

retical distributions were normalized to match the areas under the experimental curves. This normalization factor directly yields the transition strength $(2J_f+1)S_{ji}^{J'}$

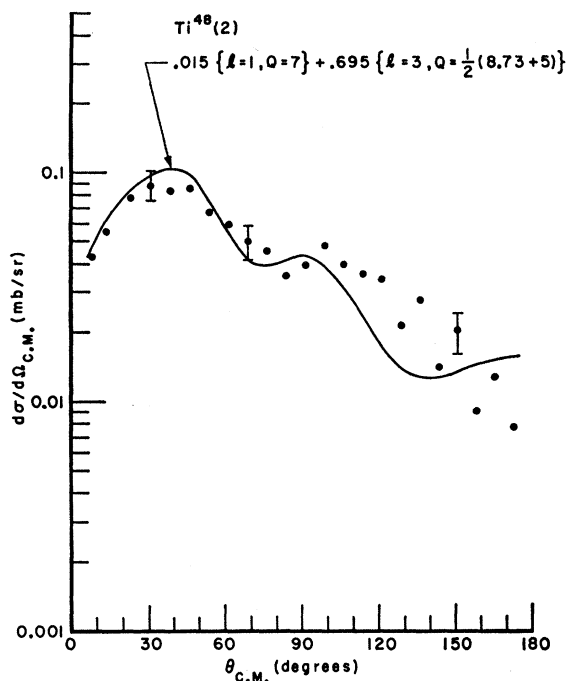


FIG. 5. Observed (d,p) distribution for the transition to $Ti^{48}(2)$. The curve is the predicted distribution obtained by adding 0.015 times the DWBA prediction for $l_n=1$, $Q=7$ to 0.695 times the average of the DWBA predictions for $l_n=3$ and $Q=8.73$ and 5 MeV. The composition of the theoretical curve is indicated in straightforward notation on the figure. The deuteron $B4$ potential is used throughout the present work.

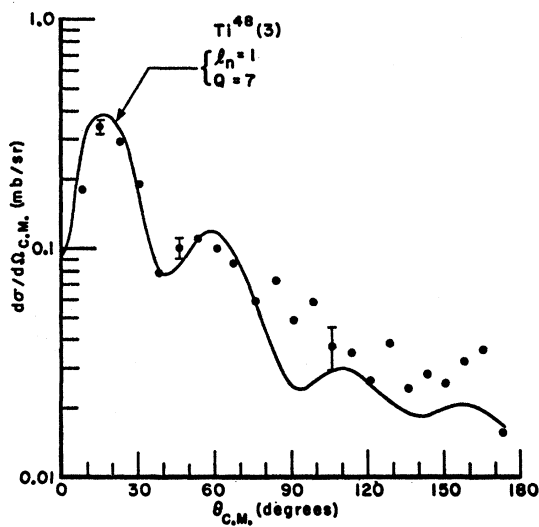


FIG. 6. Transition to $Ti^{48}(3)$. See also caption for Figs. 4 and 5.

(see also the discussion in Ref. 1). In cases where more than one l_n value is needed to obtain an acceptable fit to experiment, the relative strengths of the different contributions (that always were $l_n=1$ and 3) were judged from the experimental data at 15° and 22.5° , laboratory angle ($l_n=1$ strong; $l_n=3$ weak) and at 45° and 52.5° ($l_n=1$ weak; $l_n=3$ strong).

For a given Q value and strength, the $l_n=1$ cross section under the present conditions is 5 to 10 times larger than the $l_n=3$ cross section; hence, weak $l_n=1$ admixtures show up strongly in the angular distributions. It also follows that $l_n=3$ strengths derived from experiment in the presence of $l_n=1$ components must suffer

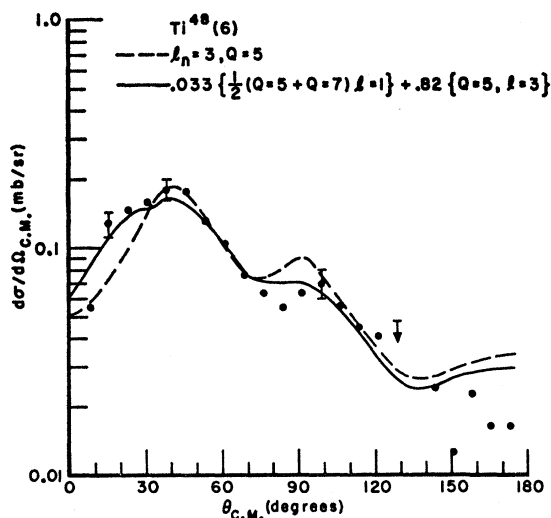
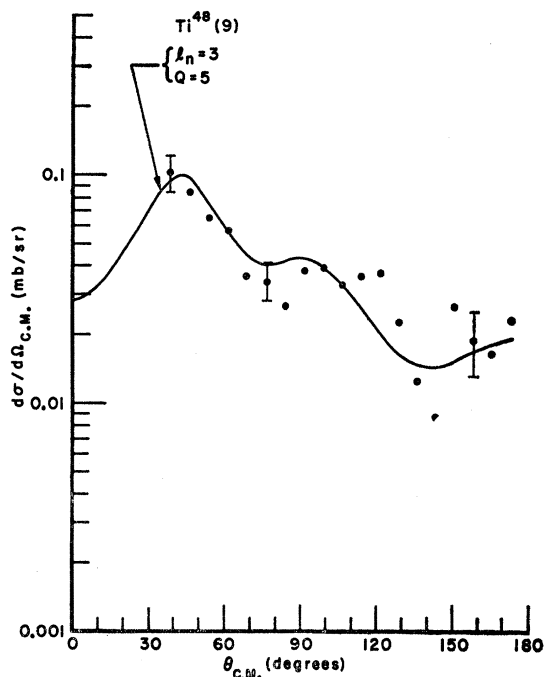
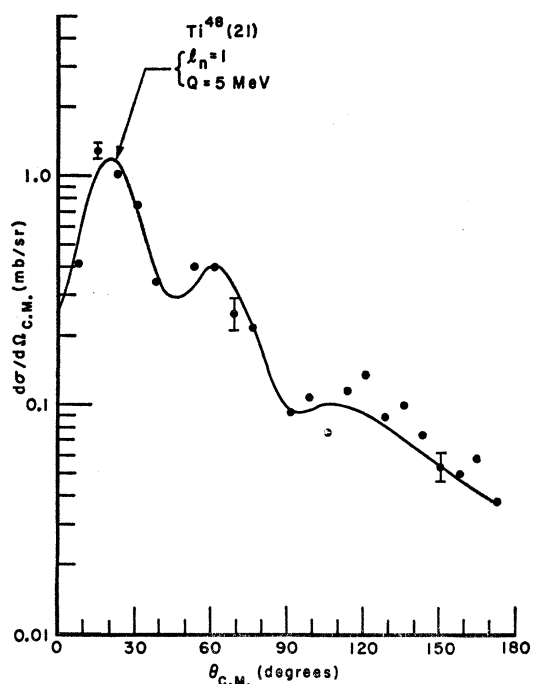
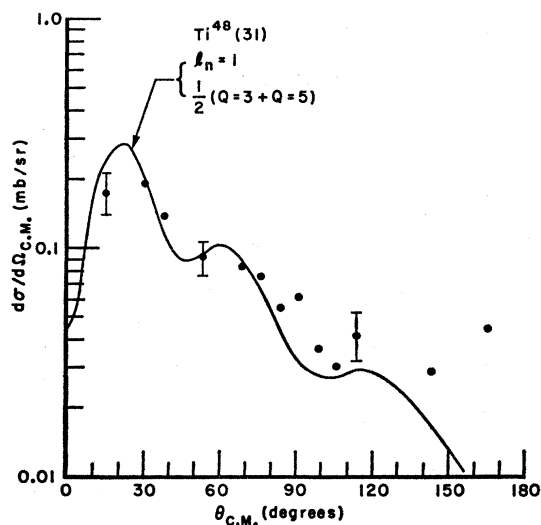
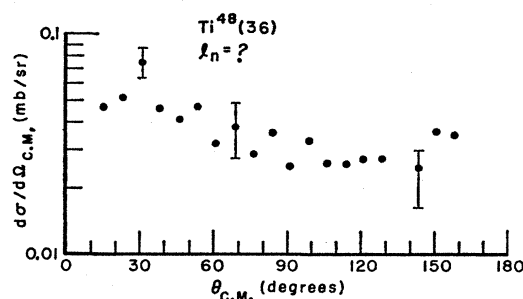
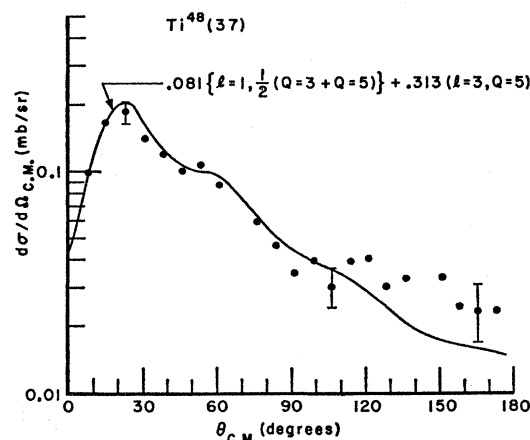


FIG. 7. Transition to $Ti^{48}(6)$, normally identified as a $6+$ state (see Table II). The $l_n=1$ admixture indicated to account for the observed (d,p) distribution precludes a $6+$ assignment for this part of the transition for reasons of angular-momentum conservation; see also the discussion in Sec. 3.1.

FIG. 8. Transition to $Ti^{48}(9)$. See also caption for Figs. 4 and 5.

rather large uncertainties. At excitation energies above approximately 5 MeV, impurity groups, background, and, in some cases, insufficient energy resolution make the quality of the data inferior to the data from lower excitation energies. Throughout the entire region of ex-

FIG. 9. Transition to $Ti^{48}(21)$. See also caption for Figs. 4 and 5.FIG. 10. Transition to $Ti^{48}(31)$. See also caption for Figs. 4 and 5.FIG. 11. Transition to $Ti^{48}(36)$. The angular distribution could not be accounted for by the distorted-wave predictions and is probably of nonstripping character. Assigned as "no unique l_n " in Table I.FIG. 12. Transition to $Ti^{48}(37)$. The first transition involving an $f_{5/2}$ neutron; cf. the discussion of Sec. IV. See also caption for Figs. 4 and 5.

citation energy covered, weak (d,p) transitions may have been missed, and above 6 MeV only the strong groups could be identified beyond doubt.

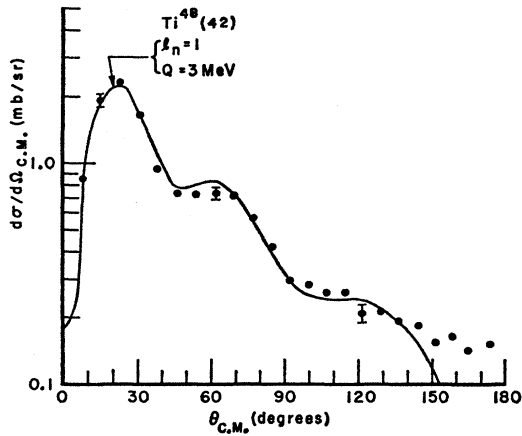


FIG. 13. Transition to $Ti^{48}(42)$. The strongest observed $l_n=1$ transition. The fit between the experimental and predicted distributions is particularly good. See also captions for Figs. 4 and 5.

The relative errors on $l_n=1$ transition strengths typically are 5 to 10%; on $l_n=3$ strengths below about 6 MeV, the relative errors are 10 to 15%; above this energy, 30 to 50%. Adding to the relative errors the uncertainty on the absolute cross-section scale of 24%, we arrive at the errors quoted in the caption for Table I. No estimate of the accuracy of the distorted-wave Born approximation *per se* has been included.

In the distorted-wave calculations, the depth of the well in which the captured neutron is supposed to move was adjusted to give to the added neutron a binding energy equal to the experimental separation energy.

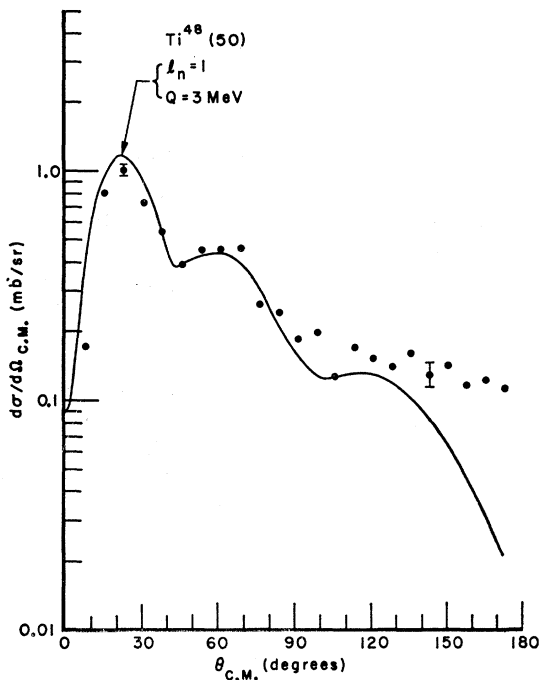


FIG. 14. Transition to $Ti^{48}(50)$. See also caption for Figs. 4 and 5.

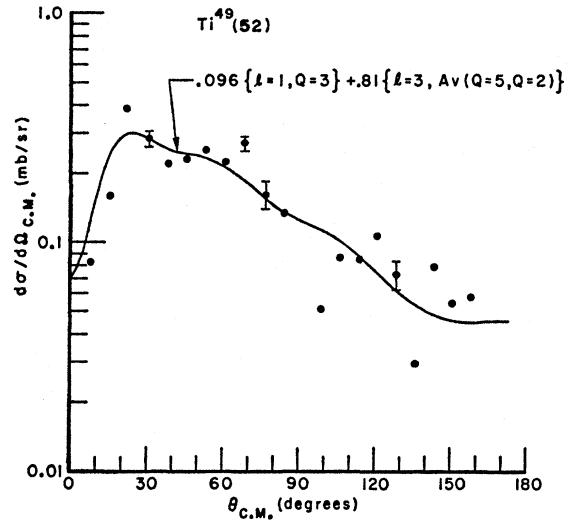


FIG. 15. Transition to $Ti^{49}(52)$. The spread of the experimental points and the quality of the DWBA fit is typical for most transitions for states higher than ≈ 6 -MeV excitation energy. The inferior fit of DWBA to experiment as compared with transitions to lower-lying states is believed to be an experimental effect. The density of proton groups on the plates is high in this range, and numerous impurity groups interfere with the Ti groups. For the notation of the figure, see captions for Figs. 4 and 5.

This procedure led to reasonable sum-rule limits in the $Ti^{50}(d, p)Ti^{51}$ case.¹ It has been pointed out,⁷ however, that even so, such a procedure may be seriously in error

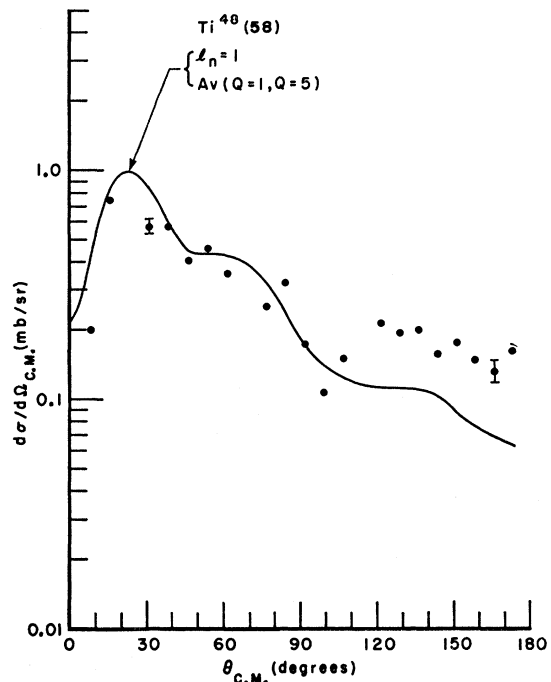


FIG. 16. Transition to $Ti^{48}(58)$. See also captions for Figs. 4 and 5.

⁷ N. Austern, Phys. Rev. 136, B1743 (1964).

TABLE I. Experimental results for the reaction $Ti^{47}(d,p)Ti^{48}$. Numbers identifying each level are given in column 1. Missing numbers mean that the corresponding level was not observed under the present conditions. (See also Sec. 3.1 and Table II). In column 2 are stated the excitation energies obtained in the present experiment as described in the text. The errors on the excitation energies are less than 12 keV. The observed $l_n=1$ and $l_n=3$ strengths are quoted in columns 3 and 4, respectively. The errors are: $\pm 25\%$ for $l_n=1$; for $l_n=3 \pm 25\%$ below 3-MeV excitation, $\pm 30\%$ up to 6 MeV, and $\pm 50\%$ above 6 MeV. No evidence for other l_n values was found. A zero in a strength column means that our data give no evidence for an admixture of the corresponding l_n value, i.e., $(2J_f+1)S_i^{J_f} < 0.3$ for $l_n=3$ and < 0.05 for $l_n=1$, respectively. An upper limit in one column and a definite strength in the other mean that the strength given was extracted from experiment under the assumption that the transition is pure; however, an admixture up to the limit given is compatible with our data. In "no unique l_n " cases, the experimental results did not allow l_n assignments. "Nonstripping" means that the measured angular distribution is incompatible with stripping theory; in most such cases the distributions are isotropic. The maximum differential cross section observed in the (d,p) transition is given by the last column.

Level No.	Excitation energy (MeV)	$(2J_f+1)S_i$		$(d\sigma/d\Omega)_{max}$ (mb/sr)	Level No.	Excitation energy (MeV)	$(2J_f+1)S_i$		$(d\sigma/d\Omega)_{max}$ (mb/sr)
		$l_n=1$	$l_n=3$				$l_n=1$	$l_n=3$	
0	0	nonstripping		0.009	40	5.563	nonstripping		0.054
1	0.983	0	12.3	0.33	41	5.636	1.04	0	0.54
2	2.299 ^a	0.06	2.8	0.085	42	5.652 ^a	4.26	0	2.31
3	2.423 ^a	1.04	0	0.34	43	5.780	no unique l_n		...
4	3.229 ^a	1.41	0	0.54	45	5.906 ^a	1.70	0	0.94
6	3.342 ^a	0.13	3.7	0.18	46	6.008	0.35	<0.5	0.13
8	3.377 ^a	0.41	<0.4	0.16	47	6.061	2.16	0	1.05
9	3.520 ^a	?	2.45	0.10	48	6.136	no unique l_n		0.13
10	3.631 ^a	0.80	0	0.29	49	6.163	0.15	0	0.12
12	3.752 ^a	0.20	2.1	0.13	50	6.332 ^a	2.11	0	1.01
15	4.048 ^a	0.57	0	0.30	51	6.381	0.84	0	0.46
16	4.087	0.29	0	0.13	52	6.509	0.38	3.28	0.38
17	4.210	no unique l_n		0.03	53	6.648	(0.29)	(0.80)	0.14
20	4.403 ^a	2.46	0	1.14	54	6.701	1.35	2.20	0.77
21	4.470	2.09	0	1.28	55	6.767	1.12	<0.5	0.40
23-24	4.595	nonstripping		0.02	56	7.250	0.54	<0.5	0.36
25	4.734 ^a	1.14	0	0.55	57	7.274	0.30	<0.5	0.20
27	4.809	0.51	0	0.23	58	7.377 ^a	1.25	0	0.74
29	4.876 ^a	0.91	0	0.47	59	7.45	1.05	0	0.73
30	4.929 ^a	0.78	0	0.38	60	7.50	no unique l_n		0.10
31	4.956	0.53	0	0.19	61	7.58	no unique l_n		0.48
33	5.015	nonstripping		0.02	62	7.73	0.49	1.00	0.50
34	5.167 ^a	1.95	0	0.93	63	7.78	0.54	<0.5	0.68
35	5.271	nonstripping		0.03	64	7.86	0.78	<0.4	0.76
36	5.319 ^a	no unique l_n		0.075	65	8.02	0.60	1.67	0.67
37	5.398 ^a	0.32	1.16	0.19	66	8.07	no unique l_n		0.37
38	5.510	0.13	0.75	0.096	67	8.11	no unique l_n		0.52
39	5.537	no unique l_n		...					

^a Energies obtained from the MIT single-gap spectrograph.

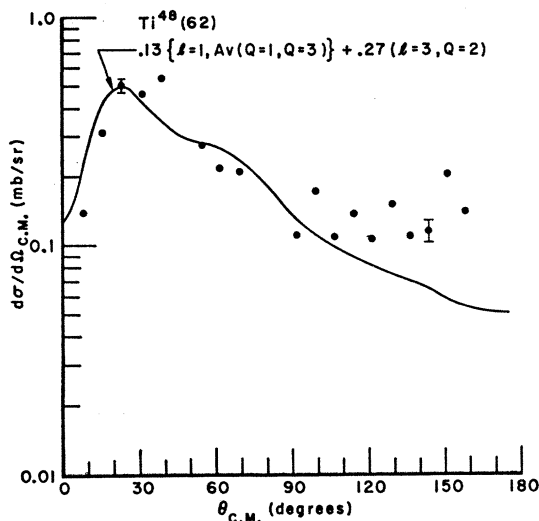


FIG. 17. Transition to $Ti^{48}(62)$. See also caption for Fig. 15.

when applied to cases where more than one l_n value is involved in a transition. Since the procedure of adjusting the well depth to yield the experimental separation energy in the present case (see Sec. IV) and in the $Ti^{49}(d,p)Ti^{50}$ case¹ again leads to reasonable sum-rule limits, we have maintained it.

The results of the present experiment are collected in Table I. Numbers identifying the levels are given in the first column. The next column contains the excitation energies obtained from measurements on selected excited states (indicated by "a") in the MIT single-gap spectrograph combined with the Q -value differences of the present experiment. The absolute Q value of the first excited state was measured as 8.439 ± 0.006 MeV, the yield of the ground state being too small to permit accurate measurement of its position. In listing the excitation energies, a value of 983 keV has been adopted for the first state. In the third and fourth columns are stated the observed $l_n=1$ and $l_n=3$ strengths, respectively; no other l_n values were observed. The maximum differential cross section measured for each group is listed in the last column.

TABLE II. Ti^{48} levels up to 5.9 MeV. Level numbers are assigned in column 1 in order of increasing excitation energy. The evidence for levels higher than level (44) comes from the present work alone (see Table I). In column 2 are listed values of the excitation energy which seem best to the present authors. For levels observed only in the high-resolution (d, p) measurements (Ref. 9 and the present experiment), the values in Table I are listed. The known spins and parities are given in column 3. The last column specifies the modes of excitation used in observing the level in question. The identification of a particular level seen in a particular experiment with a level from another experiment often is quite uncertain (cf. the discussion in the text). The general criteria for the identifications made were: (1) The levels from the different experiments should coincide energetically inside the errors given by the authors; (2) all the data on a level should be consistent, e.g., a level assigned negative parity in one experiment cannot be identified with a state showing $l_n = 1$ stripping in the present experiment.

No.	Excitation energy (MeV)	$J_f \pi$	Decay	Level reported from					No.	Excitation energy (MeV)	$J_f \pi$	Decay	Level reported from					
				(p, p')	(p, d)	(d, p)	(d, t)	$(t, p)^a$					(p, p')	(p, d)	(d, p)	(d, t)	$(t, p)^a$	
0	0	0+	b	...	e	g	i	j	23	4.591	0+	j
1	0.983	2+	b	c, d	e	c, f, g	i		24	4.595	3-	...	d	...	c, g	...	j	
2	2.295	4+	b	c, d	e	c, f, g	i		25	4.734	+	c, g	...		
3	2.423	(2)+	...	c, d	e	c, f, g	...		26	4.750	(4, 3)+	e		
4	3.229	4+	b	d	e	c, f, g	...		27	4.809	+	...	d	...	c, g	...		
5	3.240	(5+)	b		28	4.858	c		
6	3.342	6+	b	...	e	c, f, g ^h	i		29	4.876	+	g		
7	3.361	3-	...	d		30	4.929	+	...	d	...	g	...		
8	3.377	+	c, g	...		31	4.956	+	g	...		
9	3.520	(5-6)+	b	...	e	c, g	...		32	4.974	0+	j	
10	3.631	+	b	c, g	...		33	5.015	g		
11	3.710	c	...		34	5.167	+	...	d	...	g	...		
12	3.752	+	c, g	...		35	5.271	g		
13	3.793	c	...		36	5.319	g		
14	3.864	...	d	c	...		37	5.398	+	g		
15	4.048	+	d	c, g	...		38	5.510	+	g		
16	4.087	+	c, g	...		39	5.537	d	...	g	...		
17	4.210	...	d	c, g	...		40	5.563	g		
18	4.321	c	...		41	5.636	+	g		
19	4.355	c	...		42	5.652	+	g		
20	4.403	+	d	c, g	...		43	5.780	g		
21	4.470	+	c, g	...		44	5.82	d	...	g	...		
22	4.530	(4, 3)+	e		45	5.906	+	g		

^a The (t, p) data listed includes transitions to $0+$ states in Ti^{48} only.

^b Reference 8.

^c Reference 9.

^d Reference 10.

^e Reference 12.

^f Reference 4.

^g Present experiment.

^h Level (6) may be a doublet, consisting of a $6+$ state and a state with $J_f \leq 4$; the two states are less than 10 keV apart. See also the discussion in the text.

ⁱ Reference 11.

^j Reference 13.

III. COMPARISON TO OTHER EXPERIMENTS

3.1. Level Scheme

In order to investigate to what degree the Ti^{48} levels observed in the present experiment constitute a complete level scheme, we have in Table II collected all the experimental data available to us that are relevant to this question; that is, decay data⁸ and charged-particle reaction data.^{4, 9-13}

The identification of levels excited in one experiment with levels excited in another often may be difficult, as is, e.g., revealed by the situation around level num-

ber (7) (see Table II). Level (6) is known from decay data⁸ as a $6+$ state at 3340 keV. Bjerregaard *et al.*⁹ report a level at 3338 ± 12 keV from $Ti^{47}(d, p)$, and the present experiment yields a state with $l_n = 1+3$ at 3342 ± 8 keV. Recalling that the character of the target nucleus Ti^{47} is $\frac{5}{2}-$, the $l_n = 1$ admixture precludes a $6+$ assignment; possibly two close-lying levels exist (less than 10 keV apart), one of character $6+$, the other having $1 \leq J \leq 4$, with positive parity. Level (7) is given by Matsuda¹⁰ as 3361 keV, with spin and parity $3-$. A level at 3377 ± 12 keV is excited in $Ti^{47}(d, p)$, but since it has $l_n = 1$ character, and thus positive parity, it cannot be the $3-$ state of Matsuda.

The second $3-$ state observed by Matsuda corresponds energetically to a nonstripping state observed here. These two states may be the same [state (24) in Table II], but there is no strict argument for the identification suggested. The identifications between levels excited in different ways as given in Table II are all consistent with the present knowledge, but should be considered as tentative.

⁸ Landolt-Börnstein, *Zahlenwerte und Funktionen, Neue Serie I/1* (Springer-Verlag, Berlin, 1961); M. Hillman, Phys. Rev. **129**, 2227 (1963); R. A. Ristinen, A. A. Bartlett, and J. J. Kraushaar, Nucl. Phys. **45**, 321 (1963).

⁹ O. Hansen, Nucl. Phys. **28**, 140 (1961); J. H. Bjerregaard, P. F. Dahl, O. Hansen, and G. Sidenius, *ibid.* **51**, 641 (1964).

¹⁰ K. Matsuda, Nucl. Phys. **33**, 536 (1962).

¹¹ J. L. Yntema, Phys. Rev. **127**, 1659 (1962).

¹² E. Kashy and T. W. Conlon, Phys. Rev. **135**, B389 (1964).

¹³ R. Middleton and S. Hinds (private communication).

The $0+$ levels at 0, 4.591, and 4.974 MeV excited in the $\text{Ti}^{46}(t,p)\text{Ti}^{48}$ reaction¹³ either have nonstripping character or are not seen in our experiment. This may be understood if the $[\pi(f_{7/2})^2\nu(f_{7/2})^{-3}]^{5/2}$ character of the Ti^{47} ground state is taken into account (π standing for proton, ν for neutron, and $[\]^j$ for vector coupling of the spins to a resultant j); the only way in which a $0+$ state may be formed in the $\text{Ti}^{47}(d,p)\text{Ti}^{48}$ reaction is by the transfer of a neutron of spin $\frac{5}{2}$, i.e., an $f_{5/2}$ neutron. Such a $0+$ state would contain $f_{7/2}$ as well as $f_{5/2}$ components. But the addition of an $f_{7/2}$ and an $f_{5/2}$ neutron to the $0+$ ground state of Ti^{46} in the (t,p) reaction cannot lead to a spin-0 final state; thus the (t,p) and (d,p) reactions will not excite the same $0+$ states in Ti^{48} .

3.2. Spectroscopic Evidence

Deuteron stripping on Ti^{47} has been reported by Bretscher *et al.*,² Zaika and Nemets,³ and more recently by Yntema.⁴ The measurements of Refs. 2 and 3 suggest l_n values for Ti^{48} states below 4.3 MeV, and so far as levels in the present work can be identified with levels in the older work, the results are in agreement.

Yntema⁴ finds that $\text{Ti}^{48}(0)$ is not excited and that $\text{Ti}^{48}(1)$ is excited with $l_n=3$ and $S=1.1\pm 25\%$. Spectroscopic data are not given for higher states. This may be compared to our results: $\text{Ti}^{48}(0)$ nonstripping, $\text{Ti}^{48}(1)$, $l_n=3$ and $S=2.4\pm 25\%$. A disagreement in absolute strength between Yntema's results and ours were also found for the lowest $l_n=1$ transitions in the Ti^{51} case,¹ but in the opposite direction to the above disagreement. The fact that the present results are in better agreement with the expected sum-rule limits (see next section) may give some confidence to our absolute strengths.

Pickup reactions from Ti^{49} targets, producing states in Ti^{48} have been reported by Yntema¹¹ (d,t), Kashy and Conlon¹² (p,d), and Kavaloski *et al.*¹⁴ (p,d). The (d,t) experiment clearly resolves states (0), (1), and (2), and the $l_n=3$ angular distributions are in essential agreement with the more extensive (p,d) results cited in Ref. 12. For higher states the somewhat poor energy resolution encountered in the (d,t) reaction makes identification of the observed triton groups with states observed in other reactions rather unreliable. The $l_n=0$ states seen in the (p,d) reaction¹² are presumably hole states, and thus should not be excited in the (d,p) reaction, in agreement with the present results. A comparison of the $l_n=1$ and 3 groups observed in (p,d) and (d,p) is deferred for convenience to the detailed model discussions of Sec. V.

Information concerning the configuration of the Ti^{48} ground state is also available from the pickup reactions using Ti^{48} as a target.^{11,12} Both reactions reveal the presence of a $(p_{3/2})^2$ admixture.

The nonstripping character of the $\text{Ti}^{46}(d,p)\text{Ti}^{47}(0)$

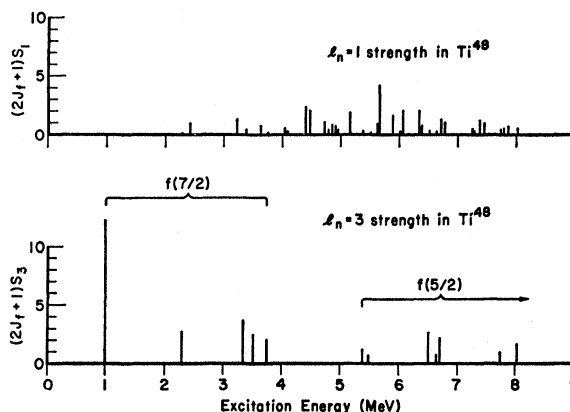


FIG. 18. Strength functions in Ti^{48} . The $l_n=1$ (d,p) strengths from Table I (upper part of the figure) and the $l_n=3$ strengths (lower part of the figure) are plotted against excitation energy. The strength is defined as $(2J_f+1)S_{ij}^{J_f}$. The contents of the figure are discussed in the text.

transition as found in Refs. 15 and 16 shows that the $\text{Ti}^{47}(0)$ state has a negligible $f_{5/2}$ single-particle strength, a conclusion confirmed in the pickup experiments.^{11,12} These experiments, however, also reveal a small $p_{3/2}$ admixture in $\text{Ti}^{47}(0)$.

Evidence on electric multipole strengths exists for the transition $\text{Ti}^{48}(0) \rightarrow \text{Ti}^{48}(1)$ which shows^{17,18} a reduced electric quadrupole transition probability $B(E2)/e^2$ of 0.031×10^{-48} cm⁴ to 0.071×10^{-48} corresponding to 6 to 14 single-particle units.¹⁹ The first $2+$ state in Ti^{48} is thus strongly excited by inelastic scattering as well as by one-nucleon transfer reactions.

IV. STRENGTH FUNCTIONS AND SUM RULES

In Fig. 18 the $l_n=1$ strengths (above) and the $l_n=3$ strengths (below) are plotted against excitation energy. It appears that the p strength ranges from 2.3 to 8 MeV without any definite grouping, whereas the f strength shows two groups, one from 1 to 3.8 MeV, and one from 5.4 and 8 MeV. We interpret the first group as corresponding to transitions in which a $1f_{7/2}$ neutron is transferred and the second group as corresponding to $1f_{5/2}$ transitions. The clear energetic separation between $1f_{7/2}$ and $1f_{5/2}$ orbits and the lack of separation between $2p_{3/2}$ and $2p_{1/2}$ orbits is in agreement with the shell-model systematics encountered in this region of elements (cf. Refs. 1 and 20).

It may also be inferred from the shell-model system-

¹⁵ J. Rappaport, Ph.D. thesis, MIT, 1963 (unpublished).

¹⁶ L. H. Th. Rietjens, O. M. Bilaniuk, and M. H. Macfarlane, Phys. Rev. **120**, 527 (1960).

¹⁷ G. M. Temmer and N. P. Heydenburg, Phys. Rev. **104**, 967 (1956); D. S. Andreyev, A. P. Grinberg, K. I. Erokhina, and I. Kh. Lemberg, Nucl. Phys. **19**, 400 (1960).

¹⁸ E. C. Booth and K. A. Wright, Bull. Am. Phys. Soc. **8**, 85 (1963).

¹⁹ K. Alder, A. Bohr, T. Huus, B. Mottelson, and A. Winther, Rev. Mod. Phys. **28**, 432 (1956).

²⁰ B. L. Cohen, R. H. Fulmer, A. L. McCarthy, and P. Mukherjee, Rev. Mod. Phys. **35**, 332 (1963).

¹⁴ C. D. Kavaloski, G. Bassani, and N. M. Hintz, Phys. Rev. **132**, 813 (1963).

atics^{20,21} that the $3s_{1/2}$, $2d_{5/2}$, and $1g_{9/2}$ states lie above the $1f$ and $2p$ states, thus giving a simple explanation of why no $l_n=0, 2$, or 4 stripping was found in the present experiment.

Some of the above conclusions may be tested quantitatively against the shell-model sum rule of French and Macfarlane²²

$$\sum_f \frac{(2J_f+1)}{(2J_i+1)} S_{ij}^{J_f} = \text{number of } (l, j) \text{ neutron holes in target.} \quad (1)$$

It was argued in the preceding section that the Ti^{47} ground state can be considered as an almost pure $f_{7/2}$ configuration with a slight p admixture. It is therefore expected that the right side of the sum rule (1) for $f_{7/2}$ neutrons is only slightly larger than 3. Correspondingly, the $p_{3/2}+p_{1/2}$ sum-rule limit is slightly less than 6, while the $f_{5/2}$ limit is 6.

In Table III the experimental and theoretical sum-

TABLE III. Sum-rule results. The experimental data shown in the first row are $(2J_i+1)^{-1} \sum_f (2J_f+1) S_{ij}^{J_f}$, where $J_i = \frac{5}{2}$. The theoretical numbers refer to the sum-rule (1) in the text.

	Number of n holes in Ti^{47}		
	$f_{7/2}$	$f_{5/2}$	$(p_{1/2}+p_{3/2})$
Experiment	4 ± 1	1.5 ± 0.5	6 ± 1
Theory	3	6	6

rule limits are compared to each other. It is seen that the $f_{7/2}$ and p strengths agree with the theoretical limits within the experimental errors, whereas only $\approx \frac{1}{4}$ of the $f_{5/2}$ strength has been detected. The results of the sum-rule analysis thus lend credence to the DWBA analysis used in obtaining the strengths of Fig. 18 and Table I.

The sums of Table III do not necessarily indicate p admixtures in the Ti^{47} ground state, although our numbers would allow an admixture of one p particle.

The sum rule for a pickup reaction corresponding to Eq. (1) is

$$\sum_f S_{ij}^{J_f} = \text{number of } (l, j) \text{ neutrons in target.} \quad (2)$$

The pickup experiment of Yntema¹¹ yields 4 ± 1 $f_{7/2}$ neutrons in Ti^{47} ; thus, the present (d, p) strength and Yntema's (d, t) strength add up to 8 particles, the total number in the $f_{7/2}$ shell. This exact agreement probably is accidental, though our $\text{Ti}^{49}(d, p)\text{Ti}^{50}$ strengths show a similar agreement with the (d, t) experiment of Yntema¹¹ [but again not with the (d, p) experiment of the same author⁴]. The (p, d) $f_{7/2}$ strength of the Ti^{47} ground state is given by Conlon and Kashy¹² as 1.8 particles, quite a low number.

²¹ B. L. Cohen, R. H. Fulmer, and A. L. McCarthy, Phys. Rev. **126**, 698 (1962).

²² M. H. Macfarlane and J. B. French, Rev. Mod. Phys. **32**, 567 (1960).

V. COMPARISON TO CURRENT NUCLEAR MODELS

5.1. The Seniority Coupling Scheme

It has been shown by Kurath and by de-Shalit and Talmi (Ref. 23) that the $v=3$ state (v standing for seniority) of spin $\frac{5}{2}$ in a $(f_{7/2})^3$ or $(f_{7/2})^{-3}$ configuration may become the lowest lying state of that configuration, provided that a residual interaction of sufficient range is present. Thus the simplest model for the Ti^{47} ground state is one in which the two extra-core protons pair their spins to 0 and the three neutron holes form a $v=3$, $J=\frac{5}{2}$ state. The corresponding Ti^{48} spectrum is that of an $(f_{7/2})^{-2}$ configuration, i.e., $v=0$, $J=0$ ground state and three excited states of $v=2$ and $J=2, 4$, and 6 , respectively. The (d, p) strengths for these states are²³ 0 for the $J=0$ ground state, 11 for the $J=2$, $v=2$ state, $12/11 \approx 1$ for the $J=4$, $v=2$ state, and $65/11 \approx 6$ for the $J=6$, $v=2$ state. Experimentally, the available $f_{7/2}$ strength is distributed over twice as many levels as predicted, and the experimental $4+$ strength is high relative to the $2+$ state by almost a factor of 3 (see Table I or Fig. 18).

An explanation for the large number of Ti^{48} states with $f_{7/2}$ strength would be to assume that excited proton configurations are present in the Ti^{47} and Ti^{48} ground states. Such a model can still be treated within the seniority coupling scheme by using wave functions of definite isospin, reduced isospin, and seniority. However, this model when applied to the present nuclei requires extra quantum numbers in addition to the above-mentioned and the spin in order to characterize the excited states. A detailed comparison to this model is therefore deferred to the simpler $\text{Ti}^{49}(d, p)\text{Ti}^{50}$ case,¹ where it was found that the model was still seriously in error, as anticipated by the work of Ginocchio and French.²⁴

5.2. The Model of McCullen, Bayman, and Zamick

The model considered by McCullen *et al.*⁵ describes the low-lying Ti states as linear combinations of $f_{7/2}$ neutron and proton configurations. They introduce an effective two-body residual interaction between pairs of nucleons in the $f_{7/2}$ shell, represented in terms of the interaction matrix elements of the one neutron-one proton configuration (Sc^{42}). The matrix elements are adjusted to reproduce the experimental excitation spectrum of Sc^{42} and are assumed to be independent of isotopic spin. For the two-proton- n -neutron problem, wave functions were obtained by a complete diagonalization of the total interaction matrix. These wave functions do not have definite seniority although they have a well-defined isospin.

The spins, parities, excitation energies,⁵ and (d, p)

²³ A. de-Shalit and I. Talmi, *Nuclear Shell Theory* (Academic Press Inc., London, 1963); D. Kurath, Phys. Rev. **80**, 98 (1950).

²⁴ J. N. Ginocchio and J. B. French, Phys. Letters **7**, 137 (1963).

TABLE IV. Comparison of our results with the calculations of McCullen, Bayman, and Zamick. In the first three columns are given the data from the present experiment on those transitions calculated by McCullen *et al.* (Refs. 5 and 25). The identification of states is believed to be consistent with that used in Ref. 5. The data for the calculated transitions are given in the last three columns; the excitation energies are taken from Ref. 5, the (d,p) strengths from Ref. 25. The experimentally observed (d,p) transition to level (12) has not been identified with any of the theoretically predicted transitions. See also the discussion in the text.

Level number	Present experiment		Theory of McCullen <i>et al.</i>		
	Excitation energy (MeV)	$(2J_f+1)S_{3,7/2}^{J_f}$	J_f, π	Excitation energy (MeV)	$(2J_f+1)S_{3,7/2}^{J_f}$
(0)	0	0	0+	0	0
(1)	0.983	12.3	2+	1.216	7.27
(3)	2.423	0	2+	2.023	2.21
(2)	2.295	2.8	4+	2.525	0.95
			3+	3.011	0.58
(4)	3.229	0	4+	3.352	0.28
(6)	3.342	3.7	6+	3.355	2.60
(9)	3.520	2.5	6+	3.486	2.71
			1+	3.831	0.43
			2+	3.970	0.16
			4+	4.347	0.52
			5+	4.581	0.09
			6+	4.967	0.37

strengths²⁵ for the first 13 states of Ti⁴⁸ as predicted by this model are given in columns 4, 5, and 6 of Table IV. The experimental data from the present experiment are given in columns 1, 2, and 3 of this table; the identification of experimental and theoretical states suggested by the table, closely follows the identifications proposed in Ref. 5. Level (12) (see Table I) which carries an appreciable $(f_{7/2})$ strength has not been identified with any theoretical level.

The Ti⁴⁸ ground state is not observed experimentally in accordance with the model predictions. The first 2+ state experimentally carries the largest $f_{7/2}$ strength, qualitatively in accordance with the model. Quantitatively the observed strength is $\approx 60\%$ larger than predicted. The observed pickup strengths to this level is ≈ 0.7 particles^{11,12} compared to a predicted value of ≈ 0.8 (see Ref. 5). The second 2+ state [state (3)] shows no $f_{7/2}$ strength in either stripping or pickup in definite disagreement with the model predictions. In (d,p) this level is observed to have an appreciable $l_n=1$ strength, i.e., a major component of this state may be pictured as the Ti⁴⁷ ground state plus a $p_{3/2}$ neutron.

The observed (d,p) strength for the first 4+ state [level (2)] is three times larger than predicted, while the experimental pickup strengths^{11,12} are somewhat smaller than calculated from the model. (d,p) and (p,d) strengths to the second 4+ states agree well with theory and so do states (6) and (9) provided both have 6+ characters. Predicted 1, 3, 4, and 6+ states with observable $l_n=3$ stripping strengths were not observed.

To sum up the above comparison to the model of McCullen *et al.*⁵ we may state the main failures of the model in predicting spectroscopic factors to be (a) the incorrect description of the second 2+ state, (b) the prediction of too many levels with observable strengths,

and (c) the omission of $p_{3/2}$ admixtures. The levels (0), (1), (2), (6), and (9) are reasonably well accounted for by the model; the low (d,p) strength and large (p,d) strength predicted and observed for level (4) are impressive.

5.3. The Aligned Coupling Scheme

Lawson²⁶ and Lawson and Zeidman²⁷ have attempted to account for the spectroscopic factors observed in the Ti (d,t) experiment of Yntema¹¹ by exploring a model in which the nucleons move in a nonspherical potential. The wave functions were generated from the Nilsson wave functions²⁸ by a projection operation. It has been shown (Ref. 5) that the ground-state wave functions so obtained to a large extent ($\lesssim 90\%$) overlap with those considered by McCullen *et al.*⁵ The predictions of the Lawson and Zeidman model were in reasonable agreement with experiment and similar to those of Ref. 5, though less detailed.

In the aligned coupling scheme^{28,29} a ground-state spin of $\frac{5}{2}-$ is predicted for Ti⁴⁷ provided a positive deformation is assumed, i.e., the odd neutron moves in a $\Omega=K=\frac{5}{2}$ orbit. Unfortunately, neither the electric quadrupole moment nor its sign are known experimentally for Ti⁴⁷, so the choice of positive deformation at least at present is an *ad hoc* one. The Ti⁴⁸ level scheme, however, does not lend itself readily to an interpretation in terms of rotational sequences.

It was found that working with three intrinsic states, $[\Omega_1=\frac{5}{2}, \Omega_2=\frac{5}{2}, K=0]$, $[\Omega_1=\frac{7}{2}, \Omega_2=\frac{5}{2}, K=1]$, and $[\Omega_1=\frac{5}{2}, \Omega_2=\frac{7}{2}, K=6]$ and assuming a sufficient Coriolis admixture^{29,30} between the first two bands, the model predicts that altogether six states would be strongly populated by $f_{7/2}$ stripping, namely the $J=2$ and 4 members of the $K=0$ band (ground-state band), the $J=1, 2,$ and 3 members of the $K=1$ band and the $J=6$ member of the $K=6$ band. No members of the $[\Omega_1=\frac{7}{2}, \Omega_2=-\frac{7}{2}, K=0]$ band will be populated. It thus seems that the main failures of the McCullen *et al.*⁵ calculation are still present, whereas almost none of its virtues survive. The Coriolis interactions needed in order to account for strengths makes the agreement between calculated and experimental excitation energies even worse than in the nonadmixed case.

5.4. Vibrational Model

The first 2+ states in even nuclei in the region of elements close to Ti have often been classified as vibrational states (see, e.g., Refs. 19 and 31). It is also pos-

²⁶ R. D. Lawson, Phys. Rev. **124**, 1500 (1961).

²⁷ R. D. Lawson and B. Zeidman, Phys. Rev. **128**, 821 (1962).

²⁸ S. G. Nilsson, Kgl. Danske Videnskab. Selskab, Mat. Fys. Medd. **29**, No. 16 (1955).

²⁹ O. Nathan and S. G. Nilsson, to appear in $\alpha, \beta,$ and γ -Ray Spectroscopy, edited by K. Siegbahn, (North-Holland Publishing Company, Amsterdam, 1964).

³⁰ A. K. Kerman, Kgl. Danske Videnskab. Selskab, Mat. Fys. Medd. **30**, No. 15 (1956).

³¹ G. Scharff-Goldhaber and J. Weneser, Phys. Rev. **98**, 212 (1955).

²⁵ B. Bayman (private communication).

sible to excite a phonon state in an even nucleus through (d, p) stripping (see, e.g., Ref. 32), but it is normally expected that the particle strength is distributed over many shell model states,³³ thus making a strong transition through one l_n value improbable. If we want to describe $Ti^{48}(1)$ as a vibrational state, it is therefore necessary to assume that most of the phonon strength is already present in $Ti^{47}(0)$. Under this assumption the $Ti^{48}(1)$ can be reached by "pairing off" the odd particle in Ti^{47} . This picture, however, is hardly consistent; first the configuration of $Ti^{47}(0)$ is almost pure $f_{7/2}$ (see Sec. 3.2); second, the coupling between particles and phonons demanded to give an appreciable phonon strength in $Ti^{47}(0)$ is so large that the concept of a definite phonon number no longer is valid, i.e., we approach the

deformed coupling scheme; third, this picture does not explain why the $J=\frac{5}{2}$ state is the ground state in Ti^{47} .

ACKNOWLEDGMENTS

We are indebted to Dr. G. R. Satchler for performing the DWBA calculations for us. Dr. B. Bayman kindly has given us access to the numerical values of the (d, p) spectroscopic factors calculated from the wave functions of Ref. 5. It is a pleasure to thank Professor Aa. Bohr and Professor B. Mottelson for their stimulating interest in the present work. The cooperation of Professor H. Enge and Professor W. Buechner is greatly appreciated.

The help of Joseph Comfort and Miss Birthe Klinskov with calculations and the careful scanning of the nuclear emulsions by Mrs. Virginia Camp, Mrs. Masako Nagatani, and Mrs. Mieko Kitajima are gratefully acknowledged.

³² S. Yoshida, Nucl. Phys. **38**, 380 (1962).

³³ B. Mottelson, *Proceedings of the International Conference on Nuclear Structure, Kingston, 1960* (University of Toronto Press, Toronto, 1960), p. 525.

Phenomenological Potentials and the $D(n, p)2n$ Reaction. II

D. R. KOEHLER

U. S. Army Missile Command, Redstone Arsenal, Alabama

(Received 28 December 1964)

Recent direct-interaction calculations of the $D(n, p)2n$ reaction cross section at 14.4 MeV have been extended to include the nucleon-nucleon potentials of Hamada and Johnston and Lassila, Hull *et al.* The calculations have been modified to incorporate the tensor potentials in the description of the final-state two-body "particles." Proton energy spectra are presented, and a comparison with previous calculations which employed the Gammel-Thaler phenomenological potentials are made. Within the present calculation framework, better agreement with the experimental results is afforded in the Gammel-Thaler and Hamada-Johnston potential descriptions than in that of Lassila, Hull *et al.*

IN a previous paper¹ the $D(n, p)2n$ reaction cross section was calculated in a direct-reaction framework utilizing the phenomenological potentials of Gammel and Thaler.² Although the approximations involved in these earlier calculations may be viewed somewhat questioningly, the results were in good agreement with the experimental data. In a recent paper by Signell and Yoder,³ several of the latest phenomenological nucleon-nucleon models were compared, and it was concluded that a "better" description was afforded, for example, by the Hamada-Johnston⁴ potentials and the Yale⁵ potentials. It was decided therefore to utilize these potentials in the calculation of the $D(n, p)2n$ reaction cross section and to note the effect on the results.

The cross-section computations were carried out in the same procedure as that of Ref. 1. By way of review, the reaction was viewed as progressing through an (n, p) mode and an (n, n') mode. The final state therefore was pictured as a continuum dineutron plus a free proton or as a continuum deuteron plus free neutron. For the interaction potential V_{int} we used $V_{int} = V_{23} + V_{13}$, where the subscripts 1 and 2 refer to the neutron and proton, respectively, in the deuteron and 3 refers to the incident neutron. The interaction potentials are, therefore, nucleon-nucleon potentials, and it is here that we employ the phenomenological potentials. In calculating the two-body continuum wave functions, however, we also use the phenomenological models.

The interaction between the two-body particle (deuteron and dineutron) and the free particle was neglected, and, furthermore, an $l=0$ approximation was used in describing the two-body particles as well as in describing the relative motion of the two-body particle and the free particle. The present calculations depart from the pre-

¹ D. R. Koehler and R. A. Mann, Phys. Rev. **135**, B91 (1964).

² J. L. Gammel and R. M. Thaler, Progr. Elem. Particle Cosmic Ray Phys. **5**, 99 (1960).

³ P. Signell and N. R. Yoder, Phys. Rev. **132**, 1707 (1963).

⁴ T. Hamada and I. D. Johnston, Nucl. Phys. **34**, 382 (1962).

⁵ K. E. Lassila, M. H. Hull, Jr., H. M. Ruppel, F. A. McDonald, and G. Breit, Phys. Rev. **126**, 881 (1962).